# Light-Induced Contraction and Extension of Single Macromolecules on a Modified Graphite Surface

Chien-Li Lee,[†] Tobias Liebig,[†] Stefan Hecht,[‡,§] David Bléger,[*,‡] and Jürgen P. Rabe[*,†,§]

[†]Department of Physics, [‡]Department of Chemistry, and [§]IRIS Adlershof, Humboldt-Universität zu Berlin, 12489, Berlin, Germany

ABSTRACT Synthetic rigid-rod polymers incorporating multiple azobenzene photoswitches in the backbone were deposited from solution onto a monolayer of octadecylamine covering the basal plane of graphite. Large contractions and extensions of the single macromolecules on the surface were induced by irradiation with UV and visible light, respectively, as visualized by scanning force microscopy. Upon contraction, the single polymer chains form more

compact nanostructures and also may move across the surface, resembling a crawling movement. We attribute the efficiency of these processes to the low mechanical and electronic coupling between the surface and polymers, the high density of azobenzenes in their backbones, and their rigidity, allowing for maximized photodeformations. The visualization of on-surface motions of single macromolecules directly induced by light, as reported herein, could help promote the development of optomechanical nanosystems.
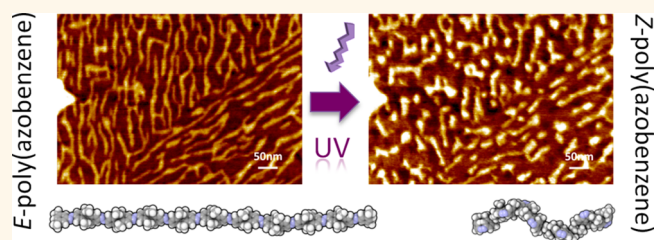
KEYWORDS: azobenzene · single macromolecule · photoisomerization · graphene · molecular workbench · scanning force microscopy

Control over the motion of single molecules is a fundamental challenge in the field of nanotechnology, in particular for the development of artificial molecular machines,[1−3] and typically requires converting external energy—either chemical fuels or physical stimuli—into movement through concerted conformational changes. Ingenious systems have been developed, sometimes inspired by Nature, such as artificial muscles[4,5] and DNA/molecular walkers,[6−9] or by our macroscopic surroundings, such as molecules resembling wheels,[10] pinions,[11] and even cars,[12−14] for which the most sophisticated example to date is a system equipped with four rotary motors fueled by electrons *via* voltage pulses.[15] Physical stimuli, which are particularly attractive, as they allow for noninvasive control with typically high spatial precision, include electrons,[15−17] mechanical manipulation *via* the tip of a scanning probe microscope,[10,11] and light.[18]

In that context, molecules able to undergo reversible conformational changes leading to large contraction and extension of their structures are of potential great interest. Small molecules, such as azobenzene photoswitches,[19] usually exhibit contractions and extensions of low amplitudes due to their limited size,[20−23] while macromolecules are more promising for obtaining mechanical movements over larger distances.[24−26] Recently, we have shown that drastic contraction/extension cycles can be induced on command in rigid-rod polymers incorporating many azobenzene photoswitches in the main-chain (see **P1**, Figure 1).[27] The embedded photoswitches act as hinges, which upon light-induced isomerization lead to reversible shrinking and stretching of the polymer backbone. One key element of the molecular design is the rigidity of the backbone, in that case, a poly(*para*-phenylene), which maximizes the photodeformation and should eventually allow for enabling large mechanical motion. Another crucial aspect of the design is the introduction of large twist angles between the azobenzene units in order to break the conjugation. This point ensures attainment of a *cis*-rich photostationary state (PSS) upon irradiation with UV light, since azobenzenes directly connected at their *para*-positions display rather *cis*-poor PSSs.[28]
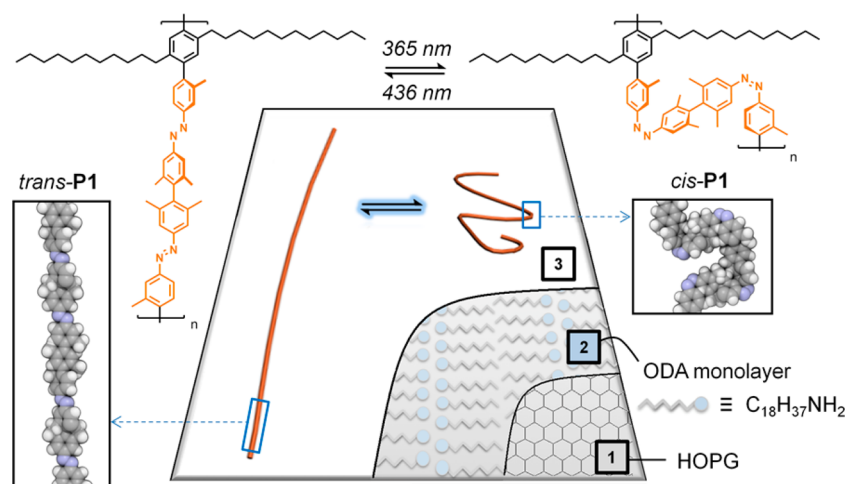
Figure 1. Chemical structure and schematic representation of P1 in the extended (*trans*-rich) and contracted (*cis*-rich) state on graphite modified with an octadecylamine (ODA) monolayer. Isolated single P1 can shrink and stretch upon exposure to UV ($\lambda = 365$ nm) and visible ($\lambda = 436$ nm) light, respectively. The three layers are labeled: 1, HOPG; 2, ODA monolayer; 3, polymer P1.

Rigid-rod polymers **P1** were shown to perform in solution, exhibiting conformational rigid-rod → random-coil transitions accompanied by changes in hydrodynamic volume of *ca.* 75%, as determined by static and dynamic light-scattering measurements. Nevertheless, in order for linear chains to eventually act as molecular machines, *i.e.*, able to transport/manipulate other objects or perform mechanical work, they arguably have to be interfaced with robust scaffolds such as nanotubes, particles, or planar surfaces.[29]

In this article, we present the immobilization and orientation of the photoshrinkable linear polymer **P1** on a modified graphite surface and provide a direct visualization of dramatic extensions, contractions, and crawling movements of single macromolecules induced by a physical, noninvasive stimulus, *i.e.*, light.[30−32] A "molecular workbench" was employed, consisting of a graphene surface of highly oriented pyrolytic graphite (HOPG) covered by an ordered monolayer of flat-lying octadecylamine (ODA), which has been used to both orient single macromolecules and manipulate them by scanning force microscopy (SFM) techniques.[33] Indeed, the ODA monolayer decouples the polymers—both mechanically and electronically—from the surface, a point of prime importance since a strong mechanical coupling would prevent the polymers from moving at all, while an electronic coupling with the semimetallic surface could impede the photoswitches from isomerizing *via* fast quenching of the photoinduced excited states.[34]

RESULTS AND DISCUSSION

Alignment of Single Rigid-Rod Polymers on Modified Graphite. Rigid-rod polymers **P1** deposited on a graphite surface coated with an ODA monolayer were imaged by SFM (Figure 2a). Some rather high protruding defects serve as markers to ascertain that all SFM images were taken at the same location. Two different aligning directions

with 60° orientation difference of the rod-like polymers **P1** mark a clear grain boundary at the top left corner, reflecting the 3-fold symmetry of the ODA lamellae under the **P1** polymers.[33,35] Many straight rod-like conformations confirm that the initial configuration of the polymer is *trans*-rich, as received from the synthesis and corresponding to the thermodynamically most stable form of azobenzene. Occasionally, some kinks within a chain as well as overlapping of different polymers were found, but overall **P1** macromolecules are aligned along the ODA lamellae located underneath. These lamellae serve as soft nanoscopic "rails", with the chemical nature of the hydrophilic head groups and the length of the alkyl chains defining a surface potential ripple, thus orienting the single polymer molecules on the surface.[33]

Interestingly, deposited **P1** polymers exhibit a rather homogeneous height of $h = 0.7 \pm 0.1$ nm, as indicated by a cross section profile (Figure 2e, along the white line in Figure 2a). The experimental height approximately matches the expected molecular width of the backbone of **P1**, as estimated by the distance between two methyl groups placed in *meta*-position on one phenyl ring; $d_{\text{methyl−methyl}} \approx 0.5$ nm. The first two rods (numbered 1 and 2 in Figure 2e) have a characteristic width of 10 nm, which is defined as the thinnest apparent width among **P1** rods, and the distance between them is *ca.* 18 nm (about three lamellae). Nevertheless, the measured widths are broadened due to the finite SFM tip radius[36] (see discussion below for more details). The third and fourth rods (3 and 4) are separated by only 12 nm (about two lamellae), where the tip of the cantilever cannot go down to the surface due to the finite radius of the SFM tip apex, explaining why these two peaks are only partially resolved. The fifth polymer has a kinked spot, resulting in a slightly larger width. Although many closely aligned parallel polymers cannot be fully
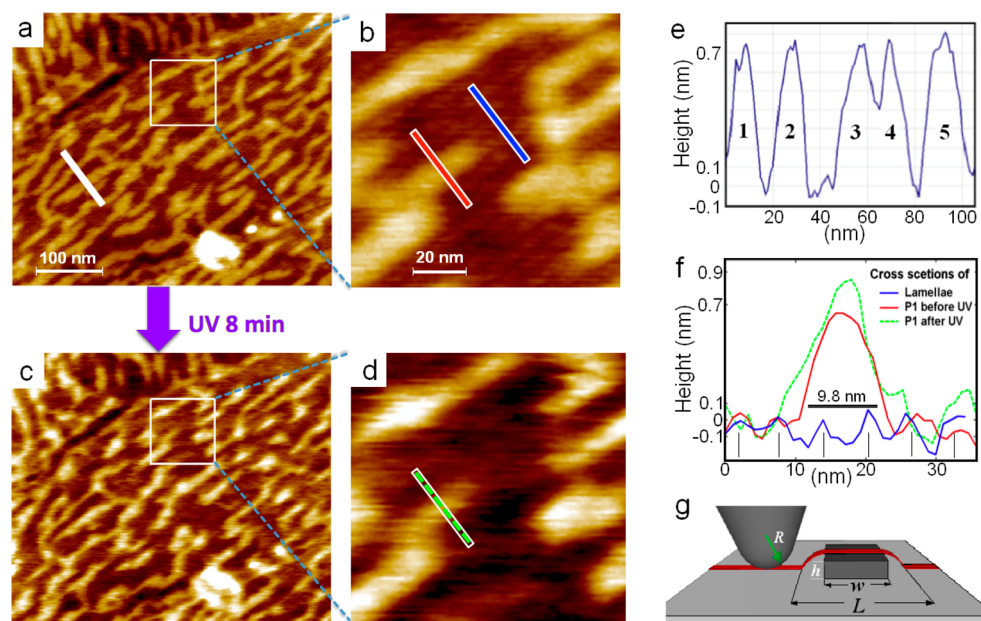
Figure 2. (a) SFM image of rod-like polymers P1 aligned along ODA lamellae before UV irradiation. (b) Zoom-in image showing that the ODA lamellae were preserved postdeposition (width 6 ± 0.2 nm) with the rod-like polymers aligned along the axes of the lamellae. (c) SFM image of the same area after 8 min of UV irradiation; (d) zoom-in image. (e) Cross section along the white line in (a) showing that P1 polymers exhibit a homogeneous height of 7 ± 1 Å. (f) Cross sections along the parallel blue and red lines in (b) and green dashed line in (d) showing a lamellar structure (width 6 ± 0.2 nm, lamellar peaks are indicated by vertical lines); the height of one rigid-rod polymer P1, centered at a "valley" of the ODA lamellae, changes from ca. 0.7 nm to ca. 0.9 nm upon UV irradiation. The black line indicating a length of 9.8 nm defines the apparent width of the polymer, as estimated from a model sketched in (g).

resolved by the SFM tip, some completely isolated rods can be identified.

Both **P1** polymers and ODA lamellar structures can be clearly seen in zoomed-in images (see Figure 2b). The blue line shows that the cross section of the lamellae (blue line in Figure 2f) exhibits periodic peaks and valleys (peaks are marked by vertical lines in Figure 2f) with the characteristic lamellae width of 6 ± 0.2 nm, which is very similar to the width prior to the deposition of **P1** (see Figure S1), indicating that the ODA monolayer was not altered by the deposition of the polymers. The red line in Figure 2b shows the cross section of a single **P1** polymer located above a valley of the lamella (see also red line in Figure 2f) with a width of ca. 10 nm.

The sample was irradiated with UV light (λ = 365 nm) for 8 min (Figure 2c). The color saturation (white) was set to 1.5 nm. One can observe that before irradiation nearly all **P1** polymers are under 1.5 nm height, whereas after irradiation, several parts of **P1** polymers exceed 1.5 nm height. Besides the increase of the height, most of the rods were also shortened. Zoom-in images in Figure 2b and d highlight a polymer chain, which was shortened after irradiation and concomitantly exhibits an increase in height from 0.7 nm to 0.9 nm (see green dashed line in Figure 2f). The increase in height accompanied by the shortening of the rods indicates a shrinking process, which should be attributed to the *trans* → *cis* photoisomerization of the embedded azobenzenes.

In order to quantify this process to some extent, the level of contraction was estimated on a large-scale image as the change in the area occupied by the polymers, which amounts to a 23% decrease (see Figure S2).

Due to the finite radius of the SFM tip apex, lateral dimensions of objects are generally overestimated, since the tip starts to interact with the imaged object before the tip apex encounters it. In order to know if the measured characteristic width could be the actual width of single polymer, the process of deconvolution was applied by using the following model (Figure 2g). We assume the cross section of a single **P1** polymer to be rectangular with a width w and height h. By assuming further that the tip is capped with a semisphere with radius R, the apparent width of a **P1** polymer can be estimated to be $L = w + 2(2Rh - h^2)^{1/2}$. Here, we took h from the apparent height, $h = 0.7$ nm, and assumed the real width to be $w = 3.3$ nm (assuming that dodecyl chains of **P1** are fully stretched, possibly on the alkyl chains of the ODA molecules). Taking $R = 8$ nm, *i.e.*, a typical tip radius, we obtained an apparent width of a single **P1** polymer to be $L = 9.8$ nm (black line in Figure 2f), which correlates well with the measured apparent width. Therefore, we attribute the **P1** rods with characteristic width to the width of single polymers. The formation of **P1** dimers and higher aggregates is in any case not likely due to the bulky, highly twisted tetramethyl biphenyl linkers present in the backbone of the polymer. In summary, based on the width, the height, and the geometry of the polymers,
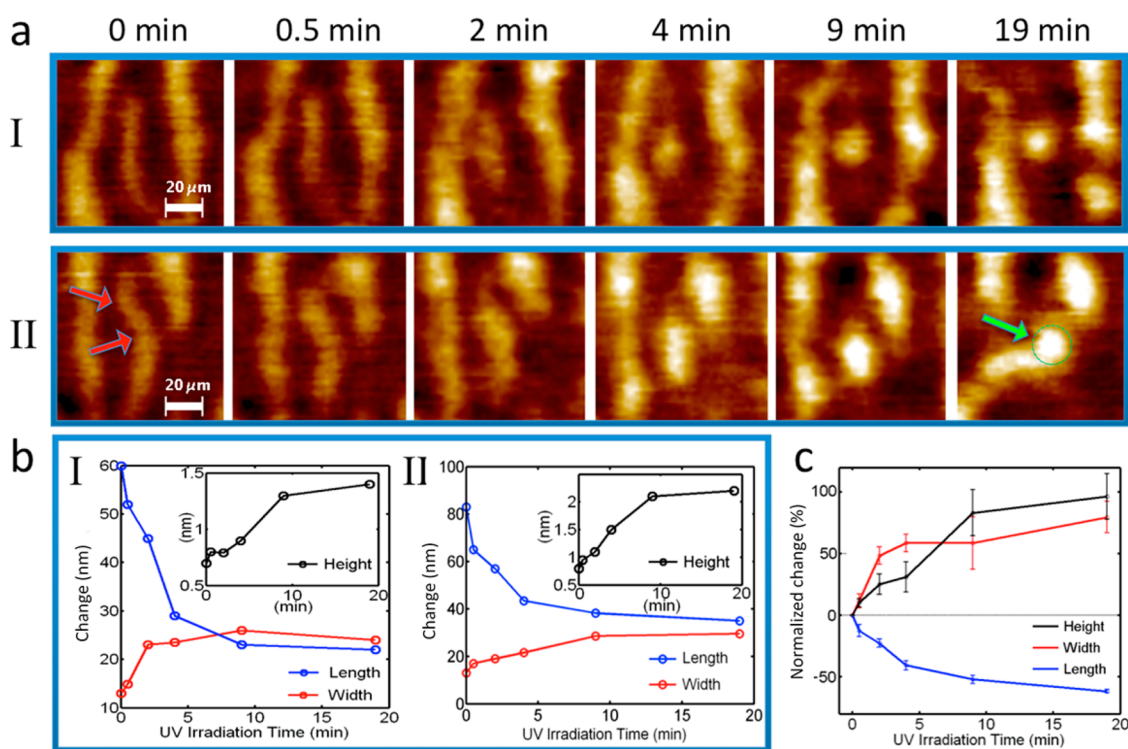
Figure 3. (a) SFM snapshots showing the shrinking of two single polymers (I and II) after UV irradiation for 30 s, 2 min, 4 min, 9 min, and 19 min (two kinks in single polymer II are indicated by red arrows). (b) Changes in length, width, and height (highest point) of polymers I and II during irradiation. (c) Normalized changes in the dimensions of the rods measured on six well-isolated single polymers with lengths ranging from 62 to 92 nm (mean values plotted with standard errors).

we can conclude that the measured rods are single (macro)molecules. This conclusion was further verified by the behavior of **P1** upon irradiation.

Light-Induced Motion of Single Macromolecules at the Surface. In a more systematic study, another sample was irradiated at $\lambda = 365$ nm for 30 s, 2 min, 4 min, 9 min, and 19 min and then at $\lambda = 436$ nm for 10 min to induce the *trans* → *cis* and back *cis* → *trans* isomerization, respectively (see Movie S1 for snapshots of **P1** polymers undergoing contractions and extensions). The width of the ODA lamellae seems to be unchanged after switching the **P1** polymers (see Figure S1), indicating that the ODA lamellae were not affected by the photoirradiation.

Figure 3a shows selected SFM zoom-in images of two different locations, following the contraction of two single rigid-rod **P1** polymers (**I** and **II**) upon UV-light irradiation. For **I** the apparent length changed from 60 nm (*ca.* 25 repeat units) to 22 nm (see Figure 3b, **I**), while the width increased from 13 nm to 24 nm and the height from 0.7 nm to 1.4 nm. After 19 min of irradiation, no further change in size was observed, indicating that the polymer reached a PSS. Both length and width attained nearly equal values, suggesting that the single chain has adopted a more compact, disk-like shape. Considering that the geometry of a single rigid-rod **P1** polymer is cylindrical, the aspect ratio can be defined as the ratio of the width to its length. Using the apparent widths and lengths,

the aspect ratio was evaluated to change drastically, from 1/4.6 to 1/1, *i.e.*, from a rod-like to a disk-like morphology. This particular change in aspect ratio was also observed in solution by light-scattering measurements.[27] Drastic contraction of $\Delta L = 38$ nm (from 60 to 22 nm) was measured in that particular case, whereas for **II**, which is longer, this value reached $\Delta L = 48$ nm (from 83 nm to 35 nm; see Figure 3b, **II**). Similar measurements performed on several other well-isolated single polymers confirm this trend; that is, upon UV-light irradiation lengths are typically reduced by about 60%, while heights and widths nearly double (see Figure 3c). The direct visualization of such high levels of *directly* light-induced contractions in single (macro)molecules is quite remarkable. It should be noted that another example of this kind, reported by Baigl and co-workers,[37] details the *indirect* light-fueled compaction of DNA, with azobenzene-containing polyamine aqueous solution acting as the photoswitchable medium; that is, the motion of the DNA at the surface was induced by structural changes of the surrounding molecules.

Besides the light-induced formation of disk-shaped single-chain polymeric nanostructures associated with the high levels of contraction, we also observed crawling movements of some polymers during UV-light irradiation. Figure 4 shows SFM snapshots of the same location (extracted from Movie S1, green frame), where a polymer, which was initially fully stretched (Figure 4a), is contracted and, at the same time, shifts
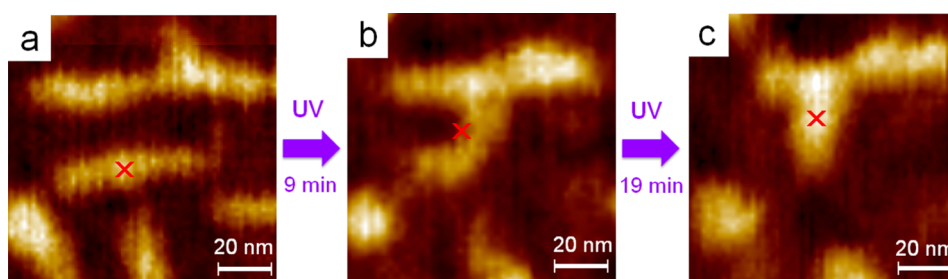
Figure 4. SFM snapshots of the same location (extracted from Movie S1, green frame) showing the crawling movement of a single P1 polymer upon UV-light irradiation for 9 and 19 min. The bending (b) and shrinking (c) of the polymer result in a translational movement, indicated by a *ca.* 10 nm shift of the center of the macromolecule (see red ×).
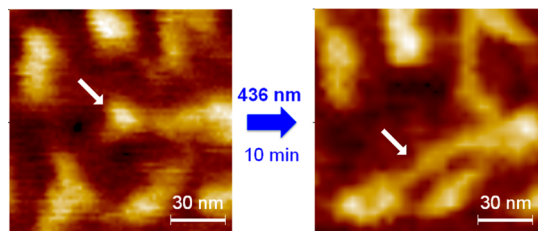
Figure 5. SFM images of the same location (extracted from Movie S1, red frame) showing a P1 disk-like polymer nanostructure that extends (see arrows) upon irradiation at λ = 436 nm for 10 min, as a result of the *cis* → *trans* isomerization of the azobenzenes in the backbone.

its center from *ca.* 10 nm (see the red cross). In the snapshot it is evident that this translation was achieved through subsequent bending and contraction of the backbone, resembling a crawling motion. This particular movement is an additional strong proof that the observed polymer is indeed a single macromolecule.

Following UV-light irradiation, we irradiated the same sample with visible (λ = 436 nm) light in order to investigate the reversibility of the process, *i.e.*, to induce the stretching of the previously contracted polymers. In a selected SFM image (Figure 5), one globular structure extends dramatically (see arrows, extended distance ~30 nm), as a result of the *cis* → *trans* isomerization of the azobenzenes. Several of

these newly extended rod-like structures can be found after blue-light irradiation, but not all the polymers could be followed individually to stretch back, since some aggregated during this process with immediate neighbors. Clearly, azobenzenes in *cis*-rich **P1** are not as photoactive as they are in the rod-like geometry of *trans*-rich **P1**, possibly due to an increased steric hindrance and lack of free volume inside the polymeric particle.

CONCLUSION

In conclusion, we demonstrated that single rigid rod-like azobenzene-containing macromolecules are immobilized, oriented, and isolated on the well-defined surface of an ODA self-assembled monolayer paving HOPG. Dramatic contraction and extension of single macromolecules on the surface were induced by irradiations with different wavelengths. The successful photoisomerization processes can be attributed to the low polymer−surface mechanical and electronic coupling obtained due to the isolating monolayer. Besides the internal motion of the polymers, light-induced crawling movement of single polymers on the surface was described, the directionality of which should be further controlled—for example through the use of polarized light and more mobile templates—in order to develop useful optomechanical nanomachines.

MATERIALS AND METHODS

Preparation and Characterization of P1 Polymers in Solution. For the purpose of reaching large-scale molecular contractions and extensions, the rigid-rod polymer **P1** (Figure 1),[27] which incorporates azobenzene photoswitches in a poly(*para*-phenylene) (PPP) backbone functionalized with dodecyl solubilizing groups, has been recently prepared by Suzuki poly-condensation and characterized in solution.[27] Large twist angles were introduced between the chromophores to break the conjugation of the π-system.[28] This electronic decoupling leads to a relatively high *cis* content in the polymeric backbone (81% upon UV-light (360 nm) irradiation in solution).[27] The molecular weight of the sample used in this study is $M_n \approx 40\,000$ g/mol, with a polydispersity index of 1.7.[38] The width of **P1** determined by the dodecyl chains (assumed stretched) is ~3.3 nm, and its height determined by the methyl groups attached to the azobenzene moieties is $d_{methyl−methyl} \approx$ 0.5 nm.

Sample Preparation and SFM Measurements. In order to isolate single rod-like **P1** polymers, the graphite surface has been modified with a SAM of octadecylamine, which has been previously demonstrated to be able to isolate and orient single macromolecules such as DNA and polyelectrolytes.[33,35] First, a droplet of octadecylamine (0.1 g/L in chloroform) was spin-coated onto freshly cleaved HOPG (ZYH grade, Materials Quartz, Inc.) at 40 rounds per second. The resulting SAM was equilibrated in water: a droplet of Milli-Q water was deposited on the surface for 15 s and removed by spinning it off. SFM images of ODA SAM reveal a lamellar structure with a width of $w = 6 \pm$ 0.2 nm (see Figure S1). In a second step, a droplet of **P1** (1 g/L in dichloromethane) was spin-casted onto the ODA monolayer. The sample was then stored in ambient conditions (white light) to allow the polymers to reach an equilibrium with the ODA monolayer. Imaging was performed by SFM in tapping mode using a multimode head (Digital Instruments Inc., Santa Barbara, CA, USA) and Olympus microcantilevers with a resonance frequency of 70 kHz and a spring constant of 2 N/m.

REFERENCES AND NOTES

1. Coskun, A.; Banaszak, M.; Astumian, R. D.; Stoddart, J. F.; Grzybowski, B. A. Great Expectations: Can Artificial Molecular Machines Deliver on Their Promise? *Chem. Soc. Rev.* **2012**, *41*, 19–30.
2. Browne, W. R.; Feringa, B. L. Making Molecular Machines Work. *Nat. Nanotechnol.* **2006**, *1*, 25–35.
3. Kay, E. R.; Leigh, D. A.; Zerbetto, F. Synthetic Molecular Motors and Mechanical Machines. *Angew. Chem., Int. Ed.* **2007**, *46*, 72–191.
4. Huang, T. J.; Brough, B.; Ho, C.-M.; Liu, Y.; Flood, A. H.; Bonvallet, P. A.; Tseng, H.-R.; Stoddart, J. F.; Baller, M.; Magonov, S. A Nanomechanical Device Based on Linear Molecular Motors. *Appl. Phys. Lett.* **2004**, *85*, 5391–5393.
5. Liu, Y.; Flood, A. H.; Bonvallet, P. A.; Vignon, S. A.; Northrop, B. H.; Tseng, H.-R.; Jeppesen, J. O.; Huang, T. J.; Brough, B.; Baller, M.; *et al.* Linear Artificial Molecular Muscles. *J. Am. Chem. Soc.* **2005**, *127*, 9745–9759.
6. Lund, K.; Manzo, A. J.; Dabby, N.; Michelotti, N.; Johnson-Buck, A.; Nangreave, J.; Taylor, S.; Pei, R.; Stojanovic, M. N.; Walter, N. G.; *et al.* Molecular Robots Guided by Prescriptive Landscapes. *Nature* **2010**, *465*, 206–210.
7. Gu, H.; Chao, J.; Xiao, S.-J.; Seeman, N. C. A Proximity-Based Programmable DNA Nanoscale Assembly Line. *Nature* **2010**, *465*, 202–205.
8. Von Delius, M.; Geertsema, E. M.; Leigh, D. A. A Synthetic Small Molecule That Can Walk down a Track. *Nat. Chem.* **2010**, *2*, 96–101.
9. Von Delius, M.; Leigh, D. A. Walking Molecules. *Chem. Soc. Rev.* **2011**, *40*, 3656–3676.
10. Grill, L.; Rieder, K.-H.; Moresco, F.; Rapenne, G.; Stojkovic, S.; Bouju, X.; Joachim, C. Rolling a Single Molecular Wheel at the Atomic Scale. *Nat. Nanotechnol.* **2007**, *2*, 95–98.
11. Chiaravalloti, F.; Gross, L.; Rieder, K.-H.; Stojkovic, S. M.; Gourdon, A.; Joachim, C.; Moresco, F. A Rack-and-Pinion Device at the Molecular Scale. *Nat. Mater.* **2007**, *6*, 30–33.
12. Shirai, Y.; Osgood, A. J.; Zhao, Y.; Kelly, K. F.; Tour, J. M. Directional Control in Thermally Driven Single-Molecule Nanocars. *Nano Lett.* **2005**, *5*, 1–5.
13. Joachim, C.; Rapenne, G. Molecule Concept Nanocars: Chassis, Wheels, and Motors? *ACS Nano* **2013**, *7*, 11–14.
14. Weiss, P. S. Nano Races, Prizes, and Awards. *ACS Nano* **2014**, *8*, 1–1.
15. Kudernac, T.; Ruangsupapichat, N.; Parschau, M.; Maciá, B.; Katsonis, N.; Harutyunyan, S. R.; Ernst, K.-H.; Feringa, B. L. Electrically Driven Directional Motion of a Four-Wheeled Molecule on a Metal Surface. *Nature* **2011**, *479*, 208–211.
16. Nickel, A.; Ohmann, R.; Meyer, J.; Grisolia, M.; Joachim, C.; Moresco, F.; Cuniberti, G. Moving Nanostructures: Pulse-Induced Positioning of Supramolecular Assemblies. *ACS Nano* **2013**, *7*, 191–197.
17. Perera, U. G. E.; Ample, F.; Kersell, H.; Zhang, Y.; Vives, G.; Echeverria, J.; Grisolia, M.; Rapenne, G.; Joachim, C.; Hla, S.-W. Controlled Clockwise and Anticlockwise Rotational Switching of a Molecular Motor. *Nat. Nanotechnol.* **2013**, *8*, 46–51.
18. Chiang, P.-T.; Mielke, J.; Godoy, J.; Guerrero, J. M.; Alemany, L. B.; Villagómez, C. J.; Saywell, A.; Grill, L.; Tour, J. M. Toward a Light-Driven Motorized Nanocar: Synthesis and Initial Imaging of Single Molecules. *ACS Nano* **2012**, *6*, 592–597.
19. Bandara, H. M. D.; Burdette, S. C. Photoisomerization in Different Classes of Azobenzene. *Chem. Soc. Rev.* **2012**, *41*, 1809–1825.
20. For the motion of single azobenzene molecules at surfaces, see for example refs 20–23: Alemani, M.; Peters, M. V.; Hecht, S.; Rieder, K.-H.; Moresco, F.; Grill, L. Electric Field-Induced Isomerization of Azobenzene by STM. *J. Am. Chem. Soc.* **2006**, *128*, 14446–14447.
21. Comstock, M. J.; Levy, N.; Kirakosian, A.; Cho, J.; Lauterwasser, F.; Harvey, J. H.; Strubbe, D. a; Frechet, J. M. J.; Trauner, D.; Louie, S. G.; *et al.* Reversible Photomechanical Switching of Individual Engineered Molecules at a Metallic Surface. *Phys. Rev. Lett.* **2007**, *99*, 038301.
22. Kumar, A. S.; Ye, T.; Takami, T.; Yu, B.-C.; Flatt, A. K.; Tour, J. M.; Weiss, P. S. Reversible Photo-Switching of Single Azobenzene Molecules in Controlled Nanoscale Environments. *Nano Lett.* **2008**, *8*, 1644–1648.
23. Dri, C.; Peters, M. V.; Schwarz, J.; Hecht, S.; Grill, L. Spatial Periodicity in Molecular Switching. *Nat. Nanotechnol.* **2008**, *3*, 649–653.
24. Hugel, T.; Holland, N. B.; Cattani, A.; Moroder, L.; Seitz, M.; Gaub, H. E. Single-Molecule Optomechanical Cycle. *Science* **2002**, *296*, 1103–1106.
25. Bléger, D.; Yu, Z.; Hecht, S. Toward Optomechanics: Maximizing the Photodeformation of Individual Molecules. *Chem. Commun. (Cambridge, U.K.)* **2011**, *47*, 12260–12266.
26. Du, G.; Moulin, E.; Jouault, N.; Buhler, E.; Giuseppone, N. Muscle-like Supramolecular Polymers: Integrated Motion from Thousands of Molecular Machines. *Angew. Chem., Int. Ed.* **2012**, *51*, 12504–12508.
27. Bléger, D.; Liebig, T.; Thiermann, R.; Maskos, M.; Rabe, J. P.; Hecht, S. Light-Orchestrated Macromolecular "Accordions": Reversible Photoinduced Shrinking of Rigid-Rod Polymers. *Angew. Chem., Int. Ed.* **2011**, *50*, 12559–12563.
28. Bléger, D.; Dokić, J.; Peters, M. V.; Grubert, L.; Saalfrank, P.; Hecht, S. Electronic Decoupling Approach to Quantitative Photoswitching in Linear Multiazobenzene Architectures. *J. Phys. Chem. B* **2011**, *115*, 9930–9940.
29. Klajn, R. Immobilized Azobenzenes for the Construction of Photoresponsive Materials. *Pure Appl. Chem.* **2010**, *82*, 2247–2279.
30. Refs 30–32 are the cases of direct visualization of macro-molecules' conformational changes induced by chemical stimuli: Kumaki, J.; Hashimoto, T. Conformational Change in an Isolated Single Synthetic Polymer Chain on a Mica Surface Observed by Atomic Force Microscopy. *J. Am. Chem. Soc.* **2003**, *125*, 4907–4917.
31. Gallyamov, M. O.; Tartsch, B.; Khokhlov, A. R.; Sheiko, S. S.; Borner, H. G.; Matyjaszewski, K.; Möller, M. Conformational Dynamics of Single Molecules Visualized in Real Time by Scanning Force Microscopy: Macromolecular Mobility on a Substrate Surface in Different Vapours. *J. Microsc.* **2004**, *215*, 245–256.
32. Kumaki, J.; Kawauchi, T.; Yashima, E. "Reptational" Movements of Single Synthetic Polymer Chains on Substrate Observed by in-Situ Atomic Force Microscopy. *Macromolecules* **2006**, *39*, 1209–1215.
33. Severin, N.; Barner, J.; Kalachev, A. A.; Rabe, J. P. Manipulation and Overstretching of Genes on Solid Substrates. *Nano Lett.* **2004**, *4*, 577–579.
34. Zhou, X.-L.; Zhu, X.-Y.; White, J. M. Photochemistry at Adsorbate/Metal Interfaces. *Surf. Sci. Rep.* **1991**, *13*, 73–220.
35. Severin, N.; Okhapkin, I. M.; Khokhlov, A. R.; Rabe, J. P. Adsorption of Polyelectrolyte Molecules to a Nanostructured Monolayer of Amphiphiles. *Nano Lett.* **2006**, *6*, 1018–1022.

36. Butt, H.-J.; Guckenberger, R.; Rabe, J. P. Quantitative Scanning Tunneling Microscopy and Scanning Force Microscopy of Organic Materials. *Ultramicroscopy* **1992**, *46*, 375–393.

37. Venancio-Marques, A.; Bergen, A.; Rossi-Gendron, C.; Rudiuk, S.; Baigl, D. Photosensitive Polyamines for High-Performance Photocontrol of DNA Higher-Order Structure. *ACS Nano* **2014**, *8*, 3654–3663.

38. As measured by GPC in THF *vs* polystyrene (PS) standards; nevertheless, owing to the rigid-rod character of PPPs, their molecular weight is most likely overestimated by a factor of 1.5−2 using GPC calibrated with flexible PS standards. See ref 39.

39. Sakamoto, J.; Rehahn, M.; Wegner, G.; Schlüter, A. D. Suzuki Polycondensation: Polyarylenes à la Carte. *Macromol. Rapid Commun.* **2009**, *30*, 653–687.